



TITLE:

Enantioselective Acetalization by Dynamic Kinetic Resolution for the Synthesis of  $\gamma$  - Alkoxybutenolides by Thiourea/Quaternary Ammonium Salt Catalysts: Application to Strigolactones

AUTHOR(S):

Yasui, Motohiro; Yamada, Ayano; Tsukano, Chihiro; Hamza, Andrea; Pápai, Imre; Takemoto, Yoshiji

---

CITATION:

Yasui, Motohiro ...[et al]. Enantioselective Acetalization by Dynamic Kinetic Resolution for the Synthesis of  $\gamma$  - Alkoxybutenolides by Thiourea/Quaternary Ammonium Salt Catalysts: Application to Strigolactones. *Angewandte Chemie* 2020, 59(32): 1347 ...

ISSUE DATE:

2020-08-03

URL:

<http://hdl.handle.net/2433/255596>

RIGHT:

This is the peer reviewed version of the following article: M. Yasui, A. Yamada, C. Tsukano, A. Hamza, I. Pápai, Y. Takemoto, *Angew. Chem. Int. Ed.* 2020, 59, 13479, which has been published in final form at <https://doi.org/10.1002/anie.202002129>. This article may be used for non-commercial purposes in accordance with Wiley Terms and Conditions for Use of Self-Archived Versions.; The full-text file will be made open to the public on 3 August 2021 in accordance with publisher's 'Terms and Conditions for Self-Archiving'.; This is not the published version. Please cite only the published version.; この論文は出版社版ではありません。引用の際には出版社版をご確認ください。

# Enantioselective Acetalization via Dynamic Kinetic Resolution for Synthesis of $\gamma$ -Alkoxybutenolide by Thiourea–Quaternary Ammonium Salt Catalysts: Its Application to Strigolactones

Motohiro Yasui,<sup>[a]</sup> Ayano Yamada,<sup>[a]</sup> Chihiro Tsukano,<sup>\*[a]</sup> Andrea Hamza,<sup>[b]</sup> Imre Pápai,<sup>\*[b]</sup> Yoshiji Takemoto<sup>\*[a]</sup>

**Abstract:** Although acetalization is a fundamental transformation in organic synthesis, intermolecular asymmetric acetalization remains an unsolved problem. In this study, a thiourea–ammonium hybrid catalyst was revealed to promote the O-alkylation of enols with a racemic  $\gamma$ -chlorobutenolide via dynamic kinetic resolution to give chiral acetals with good enantioselectivity. The catalyst simultaneously activates both the nucleophile and electrophile in a multifunctional manner. This method was applied to the asymmetric synthesis of several strigolactones. DFT calculations suggest that hydrogen bonding interaction between the chlorine of  $\gamma$ -chlorobutenolide and the Ts amide hydrogen of the catalyst, as well as other types of noncovalent catalyst–substrate interactions are crucial for achieving high stereoselectivity.

Strigolactones,<sup>[1]</sup> including strigol,<sup>[2]</sup> avenaol,<sup>[3]</sup> and GR24,<sup>[4]</sup> plant hormones that regulate root growth, have attracted substantial attention (Figure 1). They are characterized by the presence of a butenolide unit (D ring) linked to an enol through an acetal, which plays an important role in their biological activities.<sup>[5]</sup> To date, the D ring has been installed by nonselective acetalization strategies and subsequent separation of the resulting two diastereomers.<sup>[6]</sup> More efficient methods using a chiral auxiliary<sup>[7]</sup> and an asymmetric Pd-catalyzed reaction<sup>[8a]</sup> have also been devised to stereoselectively construct the chiral acetal. However, the substrate scopes of the latter methods are still unclear.<sup>[8b]</sup>

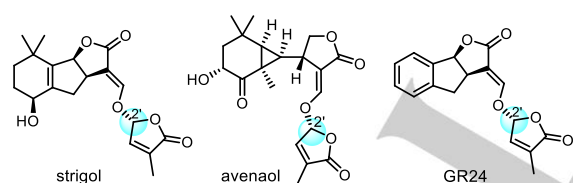


**Figure 1.** Canonical, noncanonical, and artificial strigolactones.

Acetalization is a fundamental transformation in organic chemistry<sup>[9]</sup> with various applications in the synthesis of dioxaspirocyclic natural products and polysaccharides<sup>[10,11]</sup> as well as the protection of various functional groups.<sup>[12]</sup> Acetals are generally obtained by nucleophilic addition to oxocarbenium cations or  $S_N2$ -type nucleophilic substitution reactions. When the acetal carbon is a diastereomeric center, its stereochemistry is generally controlled by neighboring group participation and conformational effects through electronic or steric interactions. In contrast, the enantioselective formation of chiral acetals from achiral compounds remains challenging. In particular, intermolecular asymmetric acetalization is limited to enzymatic reactions and Pd-catalyzed allylic substitutions.<sup>[13]</sup> However, in the last decade, a variety of elegant chemical tools for chiral acetal formation using chiral catalysts have been developed.<sup>[14,15]</sup> In 2010, List and coworkers developed an intramolecular asymmetric acetalization using a chiral phosphoric acid.<sup>[14d,e]</sup> Later, the same authors extended the method to intermolecular reactions of aldehydes with achiral and racemic diols via the corresponding oxocarbenium cations (Figure 2a).<sup>[14a,b]</sup> On the other hand, no catalytic asymmetric acetalization through an  $S_N2$ -type O-alkylation with a racemic alkyl halide has been reported. Apart from acetalization, only a few examples of asymmetric C-alkylation between prochiral enolates and secondary alkyl bromides have been developed and no  $S_N2$ -type O-alkylations have been reported.<sup>[16]</sup> We then planned an asymmetric acetalization of achiral enol **1** by O-alkylation with racemic  $\gamma$ -chlorobutenolide **2** using a chiral phase-transfer catalyst (PTC) via the kinetic resolution of **2** (Figure 2b). To obtain acetal **3** with high stereoselectivity, the catalyst would need to recognize both the nucleophile and electrophile through multipoint interactions.<sup>[17]</sup> We therefore designed a chiral thiourea–ammonium hybrid catalyst such that in the expected transition state, the thiourea and ammonium moieties of the catalyst establish multiple noncovalent contacts with an *in situ* generated enolate and both the oxygen and chlorine atoms of the butenolide, favoring the  $S_N2$ -type reaction of the enolate of **1** with one enantiomer of racemic electrophile **2**. Furthermore, if chloride anion, generated during the reaction, can promote the racemization of  $\gamma$ -chlorobutenolide **2** through a reversible  $S_N2$  reaction, dynamic kinetic resolution is expected to occur. In this report, we have developed new chiral thiourea–quaternary ammonium salts for asymmetric acetalization and applied them to the enantioselective synthesis of strigolactones as well as the determination of the absolute configuration of avenaol.<sup>[18]</sup>

[a] Dr. M. Yasui, Ms. A. Yamada, Dr. C. Tsukano,\* Prof. Y. Takemoto\*  
Graduate School of Pharmaceutical Sciences  
Kyoto University  
Yoshida, Sakyo-ku, Kyoto 606-8501, Japan  
E-mail: [tsukano.chihiro.2w@kyoto-u.ac.jp](mailto:tsukano.chihiro.2w@kyoto-u.ac.jp), [takemoto@pharm.kyoto-u.ac.jp](mailto:takemoto@pharm.kyoto-u.ac.jp)

[b] Mr. A. Hamza, Prof. I. Pápai\*  
Institute of Organic Chemistry  
Research Centre for Natural Sciences  
H-1117 Budapest, Magyar tudósok körútja 2, Hungary  
E-mail: [papai.imre@ttk.mta.hu](mailto:papai.imre@ttk.mta.hu)

Supporting information for this article is given via a link at the end of the document.

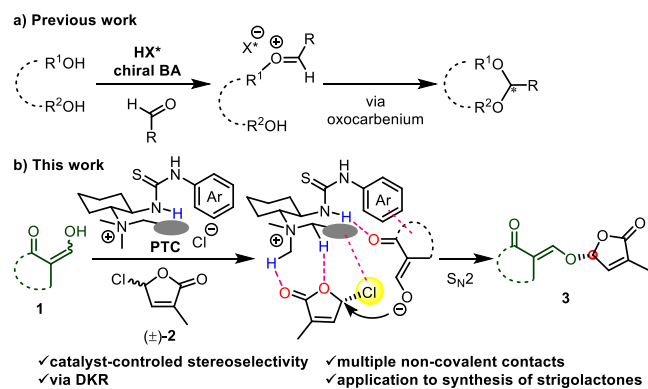
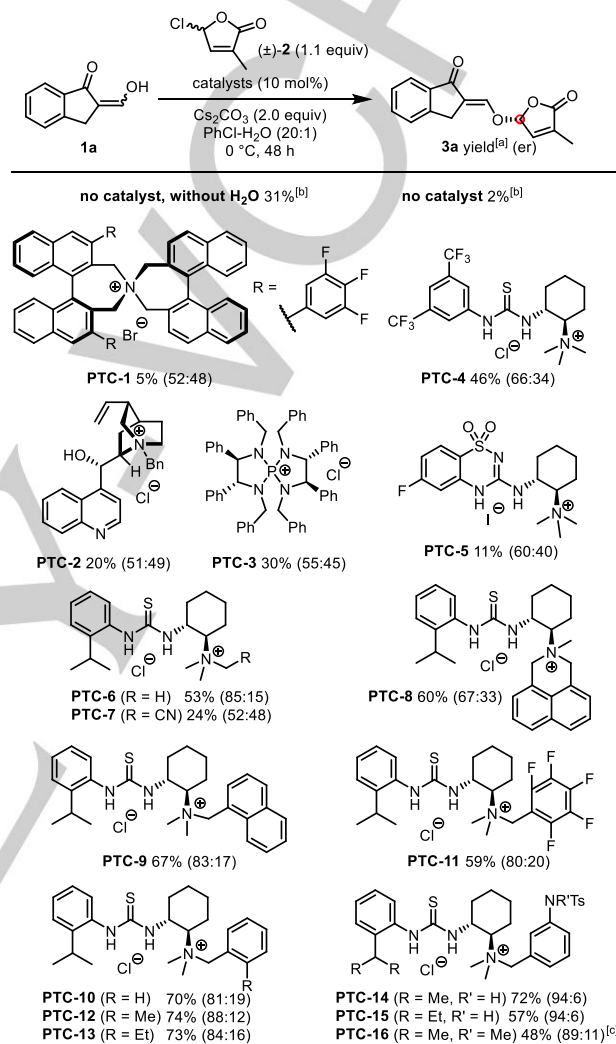


**Figure 2.** Previous studies (a) and our strategy (b) for enantioselective intermolecular acetalization.

To realize catalytic asymmetric acetalization of enol **1** by  $O$ -alkylation, we initially investigated reaction conditions to suppress the uncatalyzed reaction of **1a** with  $\gamma$ -chlorobutenolide **2** (Scheme 1). Preliminary investigations indicated that the coupling of **1a** with racemic **2** proceeded without a catalyst when cesium carbonate was used as a base in chlorobenzene. In contrast, when chlorobenzene–water (20:1, v/v) was used as the solvent, the background reaction was efficiently suppressed because the generated enolate accumulated in the aqueous phase.<sup>[19]</sup> Therefore, the same reaction was carried out in chlorobenzene–water (20:1, v/v) in the presence of various PTCs.<sup>[17b,20,21]</sup> Using spiroammonium salt **PTC-1**,<sup>[22]</sup> cinchona alkaloid derivative **PTC-2**,<sup>[23]</sup> and aminophosphonium salt **PTC-3**<sup>[24]</sup> provided desired product **3a** in 5%, 20%, and 30% yields, respectively, with low enantiomeric ratios (er). In addition, **PTC-4**,<sup>[25]</sup> bearing a thiourea moiety with a quaternary ammonium salt, gave (+)-**3a** in 46% yield with 66:34 er. Although benzothiadiazine<sup>[26]</sup> (**PTC-5**), which is a stronger hydrogen bond donor than the other catalysts, resulted in a lower yield with a similar selectivity, *o*-isopropylphenylthiourea (**PTC-6**), the bulkier hydrogen bond donor catalyst, offered greatly improved stereoselectivity (85:15 er). Regarding the substituents on the quaternary ammonium salt, the cyanomethyl group of **PTC-7** was expected to increase its hydrogen-bond-donating ability,<sup>[27a]</sup> but the use of **PTC-7** resulted in decreased selectivity. To examine the effects of the sterics of the substituents, **PTC-8**, bearing a crosslinked naphthyl group, and **PTC-9**, bearing a naphthylmethyl group, were employed, but only small effects on the yield and er were observed, as these catalysts led to 67:33 er and 83:17 er, respectively. Similarly, a series of benzyl derivatives (**PTC-10–13**) bearing benzyl, pentafluorobenzyl, *o*-tolyl, and *o*-ethylbenzyl groups afforded similar yields and selectivities. In contrast, we finally found that *m*-TsNH-benzyl catalyst **PTC-14** exhibited the best catalytic performance and gave **3a** in 72% yield with the highest selectivity (94:6 er). A comparable selectivity was obtained with **PTC-15** bearing a 3-pentanyl group instead of the isopropyl group. The reaction with **PTC-16**, bearing *m*-TsNMe-benzyl group, gave **3a** in 48% yield with 89:11. These results indicate that the NHTs group is more beneficial for the selectivity as compared to the NMeTs group. Therefore, **PTC-14** and **PTC-15** were selected as the optimum catalysts. Notably, the optimized conditions were conducted with 1.1 equiv of racemic **2**, and most of electrophile **2** was consumed. These results strongly suggest that the dynamic

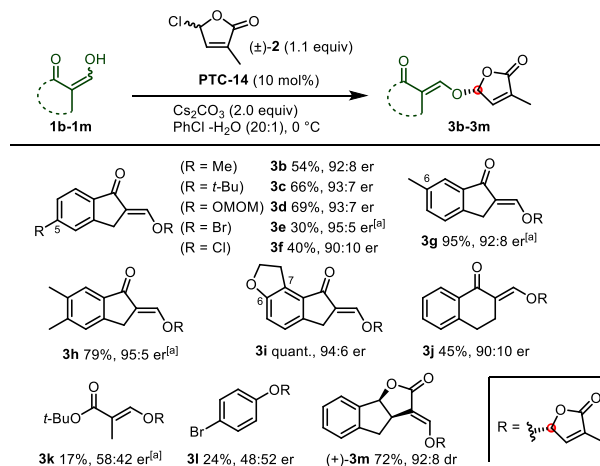
kinetic resolution of *rac*-**2** occurred during the reaction. To confirm this phenomenon, the same reaction of **1a** was performed with different equivalents of *rac*-**2** (2.0 and 4.3 equiv, also see Figure S8 in the SI).<sup>[19]</sup> In both reactions, the yields of product **3** increased with slight decreases in the er. More interestingly, the excess of electrophile **2** recovered after the reaction was nearly racemic (52:48).



**Scheme 1.** Investigation of PTC catalysts. [a] Isolated yield. [b] NMR yield using CH<sub>3</sub> as an internal standard. [c] **1a** was recovered in 24% yield.

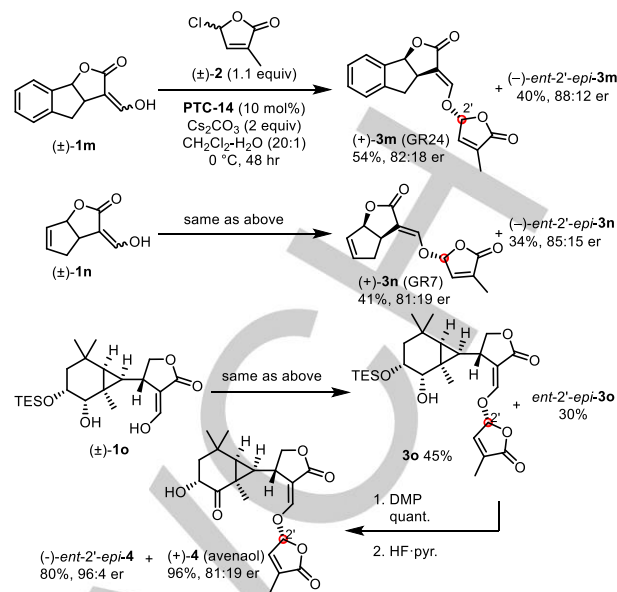
Next, the substrate scope was investigated under the optimized conditions. Several substituents were introduced at the C5 position to perturb the electron density of the enol (Scheme 2). The reaction of enols **1** bearing electron-donating groups, such as methyl (**1b**), *tert*-butyl (**1c**), and methoxymethyl (MOM; **1d**), with *rac*-**2** and a catalytic amount of **PTC-14** proceeded smoothly to furnish desired products **3b–d** in 54%–69% yields with high enantioselectivities (92:8–93:7 er). In contrast, the reaction of substrates **1e** and **1f**, bearing bromine and chlorine at C5, proceeded slowly, giving **3e** and **3f** in 30% and 40% yields with 95:5 and 90:10 er, respectively. The low yields were attributed to both the reduced nucleophilicity and low solubility of starting enols **1e** and **1f**. Products **3g–i** were

obtained in high yields with high enantioselectivities (92:8–95:5 er) from corresponding C6- and C7-substituted substrates **1g–i**. Interestingly, although the reaction of dihydronaphthalenone **1j** gave **3j** in 45% yield and comparable enantioselectivity, the same reactions with **1k** and **1l** resulted in a low yield and no selectivity. In the case of 4-bromobenzyl alcohol, no reaction occurred. These results indicated that a cyclic structure attached to the enol was important to achieve good enantioselectivity. Notably, the developed conditions were also applicable to the diastereoselective synthesis of GR24,<sup>[4]</sup> an artificial strigolactone, from enantiopure (+)-**1m** (92:8 dr).



**Scheme 2.** Scope and limitations of nucleophiles. [a] **PTC-15** was employed instead of **PTC-14**.

To demonstrate the potential of the reaction, we attempted the asymmetric syntheses of several strigolactones from racemic enols **1m** and **1n** with *rac*-**2** under the optimized conditions. From *rac*-**1m**, (+)-GR24 (**3m**)<sup>[4]</sup> was obtained in 54% yield with 82:18 er together with (–)-*ent*-2'-*epi*-**3m** in 40% yield with 88:12 er (Schemes 3 and S1 in the SI). Furthermore, the reaction of bicyclic enol *rac*-**1n** furnished (+)-GR7 (**3n**)<sup>[7]</sup> and (–)-*ent*-2'-*epi*-**3n** with comparable yields and selectivities. These results indicate that **PTC-14** precisely discriminates the chirality of  $\gamma$ -chlorobutenolide **2** but not the stereochemistry of the ring juncture in nucleophile **1**. As a general trend, **PTC-14** provides products with the (*R*)-configuration at C2' as the major isomer. Finally, we applied this reaction to determine the absolute stereochemistry of avenaol. After **PTC-14**-catalyzed introduction of the butenolide unit into *rac*-**1o**, resulting alcohols **3o** and *ent*-2'-*epi*-**3o** were converted to (+)-avenaol (**4**) and (–)-*ent*-2'-*epi*-**4**.<sup>[18]</sup> Comparing the CD spectrum of synthetic (+)-**4** with that of natural avenaol,<sup>[3]</sup> its absolute stereochemistry was determined to be 1*R*,3*S*,6*R*,7*S*,2'*R*.<sup>[28]</sup>



**Scheme 3.** Application to the asymmetric synthesis of strigolactones.

To rationalize the stereoselectivity of the observed acetalization process, we proposed the reaction mechanism depicted in Figure 3. Initially, an ion pair intermediate is formed in the water phase via the interaction of cationic catalyst **cat**<sup>+</sup> and nucleophilic enolate **en**<sup>–</sup> derived from **1a**.<sup>[19]</sup> Ion pair **cat**<sup>+</sup>/**en**<sup>–</sup> then moves to the organic phase and reacts with  $\gamma$ -chlorobutenolide **2** to afford **3a**. To elucidate the stereocontrol elements in this reaction, we computationally explored a large number of possible transition states for the  $\text{S}_{\text{N}}2$ -type substitution pathways involving **en**<sup>–</sup> and both (*R*)-**2** and (*S*)-**2** stereoisomers of  $\gamma$ -chlorobutenolide.

Our computational analysis using density functional theory (DFT) calculations<sup>[29]</sup> revealed that the enolate preferentially interacts with the *o*-isopropylphenylthiourea moiety of the catalyst (see blue arrows in Figure 3), whereas substrate **2** is activated by the tosyl-amide unit and the quaternary ammonium moiety (red arrows).<sup>[27]</sup> The most stable transition state involves concerted C–O bond formation between (*R*)-**2** and **en**<sup>–</sup> and C–Cl bond cleavage (**TS**<sup>(*R*)</sup> in Figure 3). This transition state leads to (*R*)-**3a** being the major product, and it is characterized by multiple stabilizing noncovalent catalyst-substrate interactions. Namely, the position of enolate **en**<sup>–</sup> is fixed via H-bonding interactions between the carbonyl oxygen and one of the NH groups of the catalyst's thiourea unit and via intermolecular  $\pi$ -stacking interactions.<sup>[30]</sup> On the other hand, electrophile (*R*)-**2** is bound to the catalyst by three different types of noncovalent contacts: via an N–H $\cdots$ Cl hydrogen bond involving the tosyl-amide NH group, electrostatic interaction with the positively charged ammonium unit (denoted  $\text{R}_4\text{N}^+\cdots\text{O}$  in Figure 3), and a C–H $\cdots$  $\pi$  type interaction with the aromatic ring of the tosyl group. In the reaction pathway towards (*S*)-**3a**, the minor product, the lowest lying transition state (**TS**<sup>(*S*)</sup>) is predicted to be disfavored by 1.8 kcal/mol compared to **TS**<sup>(*R*)</sup>. The enantiomeric ratio computed by considering the Boltzmann distribution of all transition state conformers is 98:2, which is in good agreement with experimental observations.

Although the enolate activation is similar in **TS**<sup>(*S*)</sup> and the N–H $\cdots$ Cl interaction between the catalyst and substrate (*S*)-**2** is

maintained, the  $R_4N^+ \cdots O^-$  and  $C-H \cdots \pi$ -type contacts are absent in this transition state due to the altered orientation of the butenolide ring. As chloride anions are present in the reaction system, fast racemization between (*R*)- and (*S*)-**2** takes place, which is also supported by computations (the barrier for the  $S_N2$ -type racemization process is predicted to be only 15.5 kcal/mol). Consequently, the dynamic kinetic resolution of *rac*-**2** would proceed to give (*R*)-**3a** as a major product. In this catalytic system, the thiourea, quaternary ammonium, and Ts amide moieties played cooperative roles in this trifunctional catalyst. This differs from Jacobsen's catalyst system,<sup>[31]</sup> because the leaving chloride anion is captured by the Ts amide moiety, not a thiourea moiety.

In summary, we have developed a novel thiourea–quaternary ammonium salt catalyst (**PTC-14**) for asymmetric acetalization. In this reaction, enantioselectivity was achieved through multiple noncovalent interactions between the thiourea, ammonium, and

Ts amide moieties in the catalyst and the enol and  $\gamma$ -chlorobutenolide. The dynamic kinetic intermolecular  $S_N2$  reaction was realized through the isomerization of  $\gamma$ -chlorobutenolide by chloride ions. This is the first example of an  $S_N2$ -type intermolecular asymmetric acetalization using an organocatalyst. This method is applicable to enantioselective and diastereoselective syntheses of strigolactones. Furthermore, the absolute stereochemistry of avenaol was determined using this method. DFT calculations of the transition states in this reaction suggested that the chlorine atom of  $\gamma$ -chlorobutenolide was activated by the Ts amide hydrogen atom, which was important for improving the selectivity. This reaction provides not only a new approach to the diastereoselective synthesis of strigolactones but also furthers our understanding of asymmetric acetalizations in which the leaving group is activated by the catalyst.

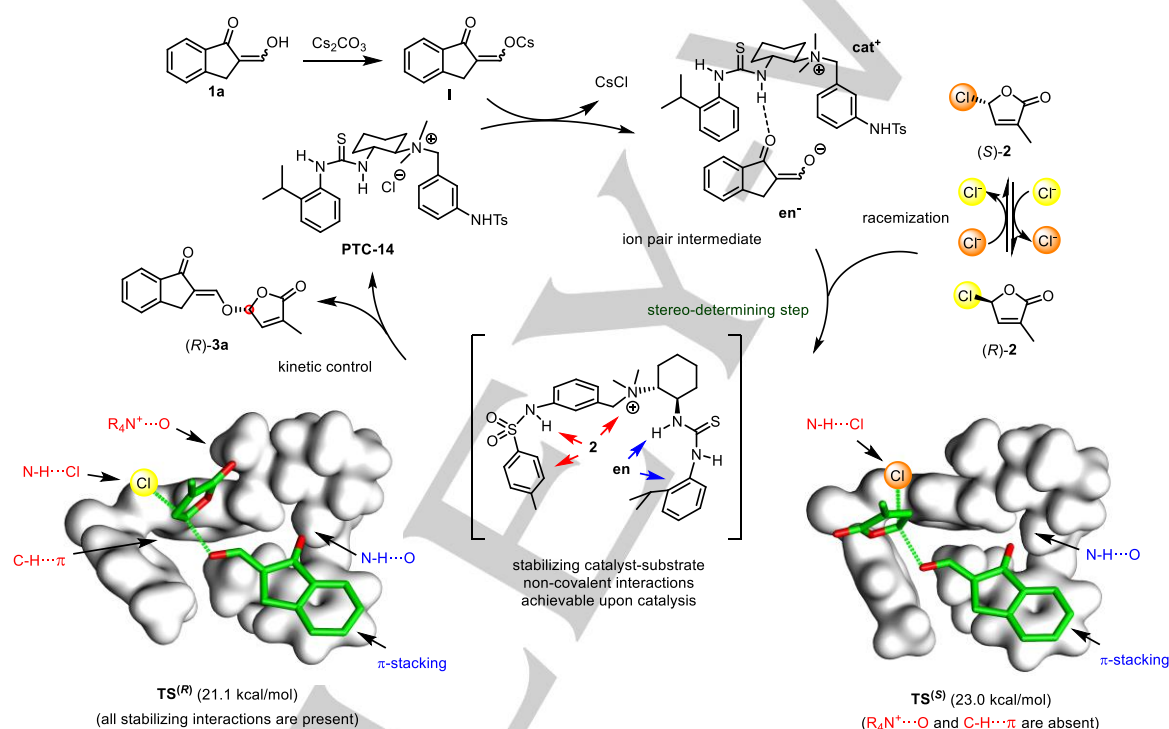


**Figure 3.** Proposed reaction mechanism and computed transition states  $TS^{(R)}$  and  $TS^{(S)}$  leading to enantiomeric products (*R*)-**3a** and (*S*)-**3a**. In the transition state structures, the catalyst framework is represented by an isodensity surface, and all hydrogen atoms in the substrates are omitted for the sake of clarity. The relative stabilities of the transition states in terms of their solvation phase Gibbs free energies (with respect to the  $cat^+/en^- + 2$  state) are given in parentheses.

## Acknowledgements

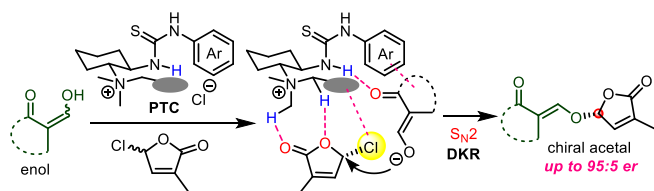
This work was supported by a Grant - in - Aid for Scientific Research (S) (JSPS KAKENHI, 16H06384, YT), a Grant - in - Aid for JSPS fellows (MY), and JSPS KAKENHI (JP17H05051 and JP18H04407, CT) in the Middle Molecular Strategy. Financial support from NKFIH Hungary (grant K-112028) and computer facilities provided by NIF HPC Hungary (project 85708 kataproc) are also acknowledged.

**Keywords:** organocatalysis • asymmetric synthesis • strigolactone • acetalization • alkylation

- [1] H. J. Bouwmeester, R. Fonne-Pfister, C. Screpanti, A. de Mesmaeker, *Angew. Chem. Int. Ed.* **2019**, *58*, 12778–12786;
- [2] a) C. E. Cook, L. P. Whichard, M. E. Wall, G. H. Egle, P. Coggon, P. A. Luhan, A. T. McPhail, *J. Am. Chem. Soc.* **1972**, *94*, 6198–6199; b) C. E. Cook, L. P. Whichard, B. Turner, M. E. Wall, G. H. Egle, *Science*, **1966**, *154*, 1189–1190.
- [3] H. I. Kim, T. Kisugi, P. Khetkam, X. Xie, K. Yoneyama, K. Uchida, T. Yokota, T. Nomura, C. McErlean, K. Yoneyama, *Phytochemistry* **2014**, *103*, 85–88.
- [4] a) A. W. Johnson, G. Gowda, A. Hassanali, J. Knox, S. Monaco, Z. Razawi, G. Roseberry, *J. Chem. Soc., Perkin Trans. 1* **1981**, 1734–1743; b) D. Uraguchi, D. K. Kuwata, Y. Hijikata, R. Yamaguchi, H. Imaizumi, A. M. Sathiyarayanan, C. Rakers, N. Mori, K. Akiyama, S. Irle, P. McCourt, T. Kinoshita, T. Ooi, T. Y. Tsuchiya, *Science*, **2018**, *362*, 1301–1305.

- [5] a) E. M. Mangnus, B. Zwanenburg, *J. Agric. Food Chem.* **1992**, *40*, 697–700; b) R. Yao, Z. Ming, L. Yan, S. Li, F. Wang, S. Ma, C. Yu, M. Yang, L. Chen, L. Chen, Y. Li, C. Yan, D. Miao, Z. Sun, J. Yan, Y. Sun, L. Wang, J. Chu, S. Fan, W. He, H. Deng, F. Nan, J. Li, Z. Rao, Z. Lou, D. Xie, *Nature* **2016**, *536*, 469–473.
- [6] L. J. Bromhead, C. S. P. McErlean, *Eur. J. Org. Chem.* **2017**, *38*, 5712–5723.
- [7] J. W. J. F. Thuring, G. H. L. Nefkens, R. Schaafstra, B. Zwanenburg, B. *Tetrahedron* **1995**, *51*, 5047–5056.
- [8] a) A. Reizelman, B. Zwanenburg, *Eur. J. Org. Chem.* **2002**, *5*, 810–814; b) L. J. Bromhead, A. R. Norman, K. C. Snowden, B. J. Janssen, C. S. P. McErlean, *Org. Biomol. Chem.* **2018**, *16*, 5500–5507; c) L. J. Bromhead, J. Visser, C. S. P. McErlean, *J. Org. Chem.* **2014**, *79*, 1516–1520.
- [9] I. Čorić, S. Vellalath, S. Müller, X. Cheng, B. List in *Topics in Organometallic Chemistry, Vol. 44*, (Eds.: L. Gooßen), Springer, Berlin, **2013**, pp. 165–193.
- [10] a) S. S. Thorat, R. Kontham, *Org. Biomol. Chem.* **2019**, *17*, 7270–7292; b) F.-M. Zhang, S.-Y. Zhang, Y.-Q. Tu, *Nat. Prod. Rep.* **2018**, *35*, 75–104.
- [11] a) M. Nielsen, C. M. Pedersen, *Chem. Rev.* **2018**, *118*, 8285–8358; b) L. Krasnova, C.-H. Wong, *J. Am. Chem. Soc.* **2019**, *141*, 3735–3754; c) H. Yao, M. D. Vu, X.-W. Liu, *Carbohydr. Res.* **2019**, *473*, 72–81.
- [12] P. G. M. Wuts, in P. G. M. in *Greene's Protective Groups in Organic Synthesis, 5th Edition; Chapter 4, Protection for the Carbonyl Group*, Wiley, Weinheim, **2014**, pp. 554–685;
- [13] a) H. van der Deen, A. D. Cuijper, R. P. Hof, A. van Oeveren, B. L. Feringa, R. M. Kellogg, *J. Am. Chem. Soc.* **1996**, *118*, 3801–3804; b) A. D. Cuijper, R. M. Kellogg, B. L. Feringa, *Chem. Commun.* **1998**, 655–656; c) B. M. Trost, F. D. Toste, *J. Am. Chem. Soc.* **1999**, *121*, 3543–3544; d) L. Jiang, T. Jia, M. Wang, J. Liao, P. Cao, *Org. Lett.* **2015**, *17*, 1070–1073.
- [14] a) J. H. Kim, I. Čorić, C. Palumbo, B. List, *J. Am. Chem. Soc.* **2015**, *137*, 1778–1781; b) J. H. Kim, I. Čorić, S. Vellalath, B. List, *Angew. Chem. Int. Ed.* **2013**, *52*, 4474–4477; c) I. Čorić, B. List, *Nature* **2012**, *483*, 315–319; d) I. Čorić, S. Müller, B. List, *J. Am. Chem. Soc.* **2010**, *132*, 17370–17373; e) I. Čorić, S. Vellalath, B. List, *J. Am. Chem. Soc.* **2010**, *132*, 8536–8537.
- [15] (a) N. Yoneda, Y. Fukuta, K. Asano, S. Matsubara, *Angew. Chem. Int. Ed.* **2015**, *54*, 15497–15500; b) Z. Sun, G. A. Winschel, A. Borovika, P. Nagorny, *J. Am. Chem. Soc.* **2012**, *134*, 8074–8077; c) Y. Khomutnyk, A. J. Argüelles, G. A. Winschel, Z. Sun, P. M. Zimmerman, P. Nagorny, *J. Am. Chem. Soc.* **2016**, *138*, 444–456; d) B. Ye, J. Zhao, K. Zhao, J. M. McKenna, F. D. Toste, *J. Am. Chem. Soc.* **2018**, *140*, 8350–8356; e) Y. Liu, Q. Chen, C. Mou, L. Pan, X. Duan, X. Chen, H. Chen, Y. Zhao, Y. Lu, Z. Jin, Y. R. Chi, *Nat. Commun.* **2019**, *10*, 1675; f) T. Yamanaka, A. Kondoh, M. Terada, *J. Am. Chem. Soc.* **2015**, *137*, 1048–1051.
- [16] a) T. Ooi, D. Kato, K. Inamura, K. Ohmatsu, K. Maruoka, *Org. Lett.* **2007**, *9*, 3945–3948; b) K. Ohmatsu, Y. Furukawa, M. Kiyokawa, T. Ooi, *Chem. Commun.* **2017**, *53*, 13113–13116.
- [17] a) D. Qian, J. Sun, *Chem. Eur. J.* **2019**, *25*, 3740–3751; b) K. Brak, E. N. Jacobsen, *Angew. Chem. Int. Ed.* **2013**, *52*, 534–561; c) M. Mahlau, B. List, *Angew. Chem. Int. Ed.* **2013**, *52*, 518–533; d) J. Novacek, M. Waser, *Eur. J. Org. Chem.* **2013**, *4*, 637–648; e) Y. Takemoto, *Chem. Pharm. Bull.* **2010**, *58*, 593–601.
- [18] M. Yasui, R. Ota, C. Tsukano, Y. Takemoto, *Nat. Commun.* **2017**, *8*, 674.
- [19] For the detailed investigation of reaction conditions and mechanisms, see the Supporting Information.
- [20] K. Maruoka in *Asymmetric Phase Transfer Catalysis*, Wiley, Weinheim, **2008**.
- [21] S. Shirakawa, K. Maruoka, *Angew. Chem. Int. Ed.* **2013**, *52*, 4312–4348.
- [22] a) T. Ooi, M. Kameda, K. Maruoka, *J. Am. Chem. Soc.* **1999**, *121*, 6519–6520; b) T. Ooi, M. Kameda, K. Maruoka, *J. Am. Chem. Soc.* **2003**, *125*, 5139–5151.
- [23] a) S. Colonna, R. Fornasier, *J. C. S. Perkin Trans. I*, **1978**, 371–373; b) S. Julia, A. Ginebreda, J. Guixer, *J. C. S. Chem. Commun.* **1978**, 742–743.
- [24] D. Uraguchi, Y. Asai, T. Ooi, *Angew. Chem. Int. Ed.* **2009**, *48*, 733–737.
- [25] Related PTCs were reported by Waser *et al.*, see: a) J. Novacek, M. Waser, *Eur. J. Org. Chem.* **2014**, 802–809; b) J. Novacek, J. A. Izzo, M. J. Veticcatt, M. Waser, *Chem. Eur. J.* **2016**, *22*, 17339–17344.
- [26] a) T. Inokuma, M. Furukawa, T. Uno, Y. Suzuki, K. Yoshida, Y. Yano, K. Matsuzaki, Y. Takemoto, *Chem. Eur. J.* **2011**, *17*, 10470–10477; b) Y. Kobayashi, Y. Taniguchi, N. Hayama, T. Inokuma, Y. Takemoto, *Angew. Chem. Int. Ed.* **2013**, *52*, 11114–11118.
- [27] a) S. Shirakawa, S. Liu, S. Kaneko, Y. Kumatabara, A. Fukuda, Y. Omagari, K. Maruoka, *Angew. Chem. Int. Ed.* **2015**, *54*, 15767–15770; b) C. Q. He, A. Simon, Y.-H. Lam, A. P. J. Brunskill, N. Yasuda, J. Tan, A. M. Hyde, E. C. Sherer, K. N. Houk, *J. Org. Chem.* **2017**, *82*, 8645–8650.
- [28] Generally, the absolute configuration of strigolactones was 2'R, and these results matched the prediction from the octant rule. For further details, see the Supporting Information.
- [29] The DFT calculations were carried out using the ωB97X-D functional along with the 6-311G(d,p) and 6-311\*\*G(3df,3pd) basis sets. The reported relative stabilities were obtained from solution phase Gibbs free energies. For details, see the Supporting Information.
- [30] Transition states involving both NH groups of the thiourea in the activation of enolate en<sup>-</sup> were also identified computationally, but they are slightly less stable as compared to TS<sup>(R)</sup>. For details, see the Supporting Information.
- [31] I. T. Raheem, P. S. Thiara, E. A. Peterson, E. N. Jacobsen, *J. Am. Chem. Soc.* **2007**, *129*, 13404–13405.

Entry for the Table of Contents



We report the development of a novel multifunctional thiourea–ammonium salt catalyst for the synthesis of chiral acetals via dynamic kinetic resolution, in which the catalyst operates as a multiple hydrogen-bond donor, coordinating with both nucleophile and electrophile. This is the first example of an  $S_N2$ -type intermolecular asymmetric acetalization using an organocatalyst.